


RESEARCH ARTICLE | MARCH 15 2023

Breathing modes of skyrmion strings in a synthetic antiferromagnet multilayer

Christopher E. A. Barker ; Eloi Haltz; Thomas. A. Moore; ... et. al

 Check for updates

Journal of Applied Physics 133, 113901 (2023)

<https://doi.org/10.1063/5.0142772>


View
Online


Export
Citation

CrossMark

Articles You May Be Interested In

Coupled breathing modes in one-dimensional Skyrmion lattices

Journal of Applied Physics (February 2018)

Microwave-induced dynamic switching of magnetic skyrmion cores in nanodots

Appl. Phys. Lett. (March 2015)

Resonate and fire neuron with fixed magnetic skyrmions

Journal of Applied Physics (October 2018)

Downloaded from http://pubs.aip.org/aip/jap/article-pdf/doi/10.1063/5.0142772/16788097/113901_1_online.pdf



Time to get excited.
Lock-in Amplifiers – from DC to 8.5 GHz

[Find out more](#)

 Zurich
Instruments

Breathing modes of skyrmion strings in a synthetic antiferromagnet multilayer

Cite as: J. Appl. Phys. **133**, 113901 (2023); doi: [10.1063/5.0142772](https://doi.org/10.1063/5.0142772)

Submitted: 17 January 2023 · Accepted: 28 February 2023 ·

Published Online: 15 March 2023



View Online



Export Citation



CrossMark

Christopher E. A. Barker,^{1,2,a)}  Eloi Haltz,^{1,b)}  Thomas. A. Moore,¹  and Christopher H. Marrows^{1,2,a)} 

AFFILIATIONS

¹School of Physics and Astronomy, University of Leeds, Leeds LS2 9JT, United Kingdom

²Bragg Centre for Materials Research, University of Leeds, Leeds LS2 9JT, United Kingdom

^{a)}Authors to whom correspondence should be addressed: pyceab@leeds.ac.uk and c.h.marrows@leeds.ac.uk

^{b)}Present address: Université Sorbonne Paris Nord, 99 Av. Jean Baptiste Clément, 93430 Villetaneuse, France.

ABSTRACT

Skyrmions are small topologically protected magnetic structures that hold promise for applications from data storage to neuromorphic computing and they have been shown to possess internal microwave frequency excitations. Skyrmions in a synthetic antiferromagnet have been predicted to be smaller and faster than their ferromagnetic equivalents and also shown to possess more internal modes. In this work, we consider the breathing modes of skyrmions in a four repetition synthetic antiferromagnetic multilayer by means of micromagnetic simulations and examine the further splitting of the modes into different arrangements of out-of-phase, in-phase, and modes with more complex phase relationships. This results in a lowering of frequencies, which is promising for skyrmion sensing applications in a synthetic antiferromagnet.

© 2023 Author(s). All article content, except where otherwise noted, is licensed under a Creative Commons Attribution (CC BY) license (<http://creativecommons.org/licenses/by/4.0/>). <https://doi.org/10.1063/5.0142772>

I. INTRODUCTION

Magnetic skyrmions are topologically protected magnetization textures where the core spin orient antiparallel to the surrounding magnetization.^{1,2} They are stabilized in bulk materials by the Dzyaloshinskii–Moriya interaction (DMI) at a narrow range of temperatures just below the ferromagnetic ordering temperature.^{3–5} In magnetic thin films, they can be stabilized at room temperature by a competition between perpendicular magnetic anisotropy, the exchange interaction, and the DMI across an interface between a magnetic layer and a non-magnetic heavy metal layer.^{6,7} It has been proposed that they could be the “bits” in a new generation of magnetic storage devices,⁸ and their fundamental properties are of great interest.⁹ There remain, however, some key challenges in applying skyrmions to real devices. Reducing their size, enhancing their robustness at room temperature, and lowering the power required to manipulate them are all active areas of research.^{10,11}

In order to overcome these challenges, it has been proposed to use synthetic antiferromagnets (SAFs).¹² In such a system, two ferromagnetic layers are coupled antiferromagnetically through a non-magnetic spacer layer in an RKKY-style interaction. Skyrmions in these systems have been predicted to be smaller,

more stable, and require less energy to manipulate.^{13,14} Recent experiments have also shown that skyrmions can be stabilized¹⁵ in such materials, and—in the case of large skyrmion bubbles—driven by applied current pulses.¹⁶ However, new challenges are introduced. Because of the cancelation of the stray field, imaging or sensing skyrmions in these systems is challenging.

Skyrmions also possess dynamic modes in the microwave frequency range. They either gyrate (rotational modes) or coherently expand and contract (breathing modes) about their center of mass. These modes are well understood both theoretically¹⁷ and experimentally^{18,19} in bulk systems and are used routinely to characterize the extent of the skyrmion pocket in phase space.²⁰ In thin film systems, this is much more difficult because of the lowered sensitivity of measurements and the reduced number of skyrmions in the system,^{21,22} and so most work on these systems is theoretical.^{23,24} It was recently shown that in synthetic antiferromagnets, the coupling between the skyrmions in each layer produces a splitting of both the rotational²⁵ and breathing²⁶ modes into in-phase (IP) and out-of-phase (OOP) modes. This is of interest because in the out-of-phase mode, one skyrmion is at its maximum radius while the other is at its minimum, so a measurable trace can be observed

in the GHz response of the system, unlike for the in-phase mode. On this basis, it has been proposed that a broadband ferromagnetic resonance (FMR) would be a robust tool to detect and identify chiral magnetic textures in a SAF.²⁷

In this work, we study the breathing modes of skyrmions in SAFs using the micromagnetic solver MUMAX3²⁸ and expand on previous work to consider SAFs with multiple repeats. In these systems, a “string” of skyrmions can be stabilized consisting of skyrmions of alternating polarity in each layer. Such skyrmion strings in SAFs have been studied under current induced motion²⁹ but their internal dynamics have never been resolved. In such samples, we see the further splitting of modes, revealing a variety of complex phase relationships and yielding resonances at lower frequencies more accessible by conventional laboratory equipment, paving the way to the experimental observation of such modes.

II. METHODS

In this study, we model our system using the finite difference micromagnetic solver MUMAX3. This numerically solves the Landau–Lifshitz–Gilbert (LLG) given by

$$\frac{d\mathbf{m}}{dt} = -|\gamma_0|\mathbf{H}_{\text{eff}} \times \mathbf{m} + \alpha\mathbf{m} \times \frac{d\mathbf{m}}{dt}. \quad (1)$$

Here, \mathbf{m} is the unit vector of the magnetization, γ_0 is the gyromagnetic constant, and \mathbf{H}_{eff} is the effective magnetic field,

$$\mathbf{H}_{\text{eff}} = -\frac{1}{\mu_0 M_s} \frac{\delta U}{\delta \mathbf{m}}, \quad (2)$$

which is proportional to the variation in the total micromagnetic energy U . M_s is the total saturation magnetization and μ_0 is the permeability of free space. U contains terms describing the Zeeman energy, the isotropic exchange interaction, demagnetization effects, a uniaxial anisotropy perpendicular to the plane of the film, and an interfacial Dzyaloshinskii–Moriya interaction (DMI), whose energy density is given by

$$U_{\text{DMI}} = D[m_z(\nabla \cdot \mathbf{m}) - (\mathbf{m} \cdot \nabla)m_z], \quad (3)$$

where D is the DMI constant and controls the strength of the interaction. The system is composed of four magnetic layers of thickness 1 nm separated by nonmagnetic spacer layers also of thickness 1 nm. Each magnetic layer is coupled antiferromagnetically to both the one above and below it in such a way that in the ground state of the system, the magnetization of the layers alternates up the stack. A schematic of the stack is shown in Fig. 1(a). Each layer is a $100 \times 100 \text{ nm}^2$ square composed of 64 cells such that the x – y cell size is 1.5625 nm, suitably smaller than the exchange length for this system $l_0 = 4.34 \text{ nm}$. The magnetic parameters of the system are defined explicitly within the simulation, with the saturation magnetization $M_s = 0.796 \times 10^6 \text{ A/m}$, exchange stiffness $A = 15 \times 10^{-12} \text{ J/m}$, uniaxial anisotropy $K = 1 \times 10^6 \text{ J/m}^3$, interfacial Dzyaloshinskii–Moriya interaction $D = 3 \times 10^{-3} \text{ J/m}^2$, and Gilbert damping parameter set to $\alpha = 0.01$ in order to resolve the

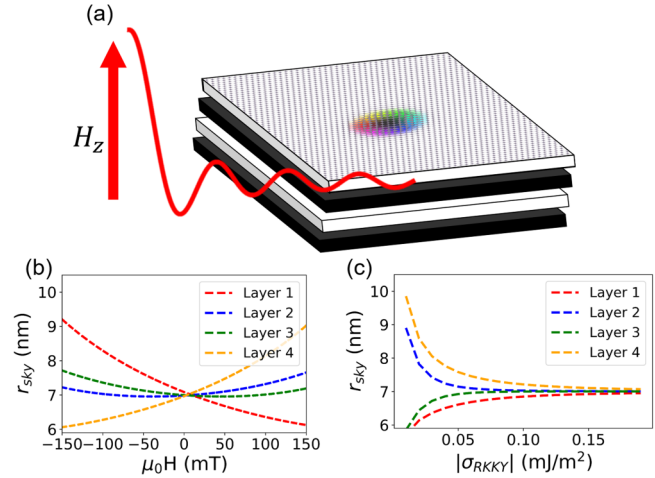


FIG. 1. (a) Schematic of the magnetic system considered along with an illustration of the out of plane sinc excitation pulse. (b) and (c) Radius of the skyrmions in each layer as a function of (b) applied magnetic field at an RKKY strength of 0.2 mJ/m^2 and (c) interlayer RKKY coupling strength in an applied field of 50 mT.

high-frequency dynamics of the system. These values were chosen to represent typical material parameters of systems shown to host skyrmions in the literature.⁷ Periodic boundary conditions were applied in order to eliminate any edge effects from the borders of the simulation and, thus, any ferromagnetic resonances of the individual layers.

The simulation was prepared with a Néel skyrmion initialized in the center of each layer of alternating core orientation and chirality. The entire system was then allowed to relax to its energy minimum with (unless otherwise specified) a static magnetic field $H_0 = 50 \text{ mT}$ applied along the positive z direction. Once the skyrmions reach their equilibrium size [shown in Figs. 1(b) and 1(c)], an oscillating H_z field was applied starting at $t = 0$ of the form

$$H_z = H_0 + \frac{H_1 \sin(2\pi f_{\text{MAX}} t)}{2\pi f_{\text{MAX}} t}, \quad (4)$$

where H_1 is the amplitude of the excitation field is set to 0.5 mT and f_{MAX} is the cut-off frequency of the excitation field is 100 GHz . This function was chosen as it is a square in the frequency domain and so excites all frequencies up to the cut-off frequency equally. After this excitation pulse, the system was allowed to run for 20 ns with the total magnetization of the system as well as the magnetization of each individual layer recorded every 2 ps. In order to calculate the frequency response of the system, we use the power spectral density (PSD), which is calculated using Eq. (5) and is the Fourier transform of the variation of the magnetization multiplied by its complex conjugate,

$$\text{PSD} = \left| \int_0^{t_0} dt \exp(2\pi i f t) \delta m_z(t) \right|^2. \quad (5)$$

The variation of the magnetization as a function of time in this expression is given by $\delta m_z(t) = \langle m_z(0) \rangle - \langle m_z(t) \rangle$, which is the difference between the spatial average of the magnetization at $t = 0$ and a given time t .

III. RESULTS AND DISCUSSION

A. Static properties of skyrmions in a SAF

In order to support our understanding of the variation of breathing modes of skyrmions in a SAF, we first consider their static properties. Figures 1(b) and 1(c) show the variation in the radius of the skyrmions as a function of an applied magnetic field (b) and strength of the RKKY interaction (c). Skyrmion radius is calculated as half the distance between zero crossings of the z component of the magnetization. As the magnetic field increases, the size of the skyrmions in the two layers whose cores align with the field also increases, as we might expect. However, as we see in Fig. 1(b), while the size of the outermost two skyrmions initially decreases, the two in the inner layers reach a minimum before increasing in size again. This is a result of being sandwiched between two increasing skyrmions and the desire of the system to exist in a state where spins in alternating layers are equal and opposite across all space, which cannot be satisfied if the skyrmion were to simply decrease in radius. Thus, the competition between the RKKY interaction and the Zeeman energy results in the skyrmion also increasing in size. In the case of the skyrmion in the outer layer, this competition also takes place but is considerably weaker as it is only affected by one nearest neighbor, so it continues to decrease in size, albeit at a decreasing rate as the RKKY energy barrier increases with an increasing disparity in skyrmion radius. The radius of the skyrmions as a function of the antiferromagnetic coupling strength was also calculated from the simulation outputs in a 50 mT static biasing field along the z axis. For suitably weak RKKY strengths, σ_{RKKY} , the radii of the skyrmions diverge due to the Zeeman interaction; however, as the strength of the RKKY increases, the radii converge to the same size which remains constant for all larger σ_{RKKY} . For all further results, unless otherwise specified, an RKKY coupling strength of $\sigma_{\text{RKKY}} = -0.2 \text{ mJ/m}^2$ was chosen; thus, in the static condition, the radii of all skyrmions are equal.

B. Dynamics

The power spectral density of the system is shown in Fig. 2 when excited by a sinc pulse in a $H_0 = 50 \text{ mT}$ biasing field. The black curve shows the frequency response of the total system, whereas those of the individual layers are shown in the other colors. Peaks are labeled as a–d to correspond to the same panels of Fig. 3. At peak (a), a strong response is observed in each of the individual layers, whereas the response of the total system is several orders of magnitude lower at this frequency. This suggests that at this peak, each skyrmion is breathing in phase with all of the others; thus, over all space the net magnetization of the system remains constant and so there is very little trace of the breathing mode. The small peak can be explained by the presence of the static biasing field inducing small differences in the sizes of the skyrmions, thus allowing us to see a (albeit small) trace of the

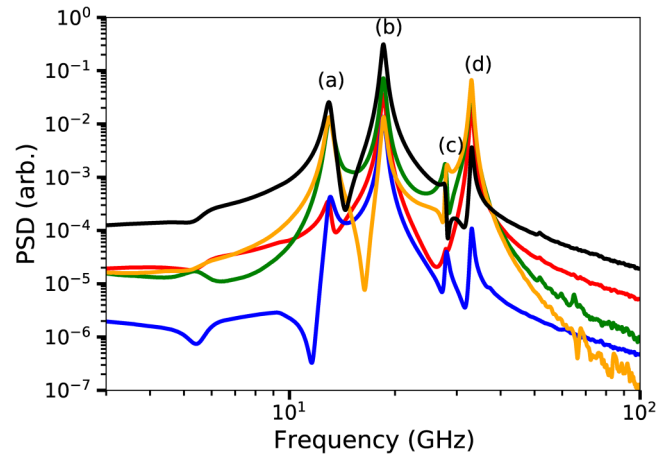


FIG. 2. Power spectral density of the SAF multilayer system after the application of sinc field pulse at $t = 0$ in a static field of 50 mT. The frequency response of the total system is plotted in black along with the individual layers in color. Labels (a)–(d) identify features of interest that correspond to Fig. 3.

breathing mode. On the other hand, at peak (b), we see a strong response in the total system as well as in each of the individual layers, suggesting an inverse relationship between the breathing modes of each layer, meaning the system oscillates between a net positive and net negative moment and there is a detectable signal. Similarly, for the two higher frequency peaks [(c) and (d)], there is almost no discernible trace of the first peak in the response of the total system, whereas there is a very strong signal for the second.

This interpretation is confirmed in Fig. 3, which shows the variation in the radius of the skyrmions in each layer when driven by a sinusoidal driving field at the frequency of each of the peaks in Fig. 2 and capturing the magnetization at intervals of 2 ps. Panels (a)–(d) correspond to the peaks labeled (a)–(d) in Fig. 2. Points correspond to the measured radius of the skyrmions, whereas solid lines are fits to a general sinusoidal function of the form $F(t) = I \sin(2\pi ft - \phi)$. Values of the phase corresponding to all of these fits are shown in Table I, which aid in our interpretation of panel (c), in particular. There we see that the phase varies by approximately $\pi/4$ between each layer, in such a way that if we consider a vertical slice through the system, the total magnetization remains essentially unchanged, hence resulting in there being no features present in the PSD of the entire system.

This more complex behavior compared to the simple system presented in Ref. 26 can be explained by considering the symmetry breaking of the system.³⁰ Each additional skyrmion in the system increases the number of possible arrangements of the breathing modes, as would be expected for any system of coupled harmonic oscillators. The ordering of the mode frequency is in order of energy minimization, where in our systems, the dominant interaction is the RKKY-style antiferromagnetic coupling. Thus, the lowest energy mode is the one where the skyrmions breathe in phase with the same amplitude, as, thus, the total magnetization through the system remains constant at all time t and the RKKY

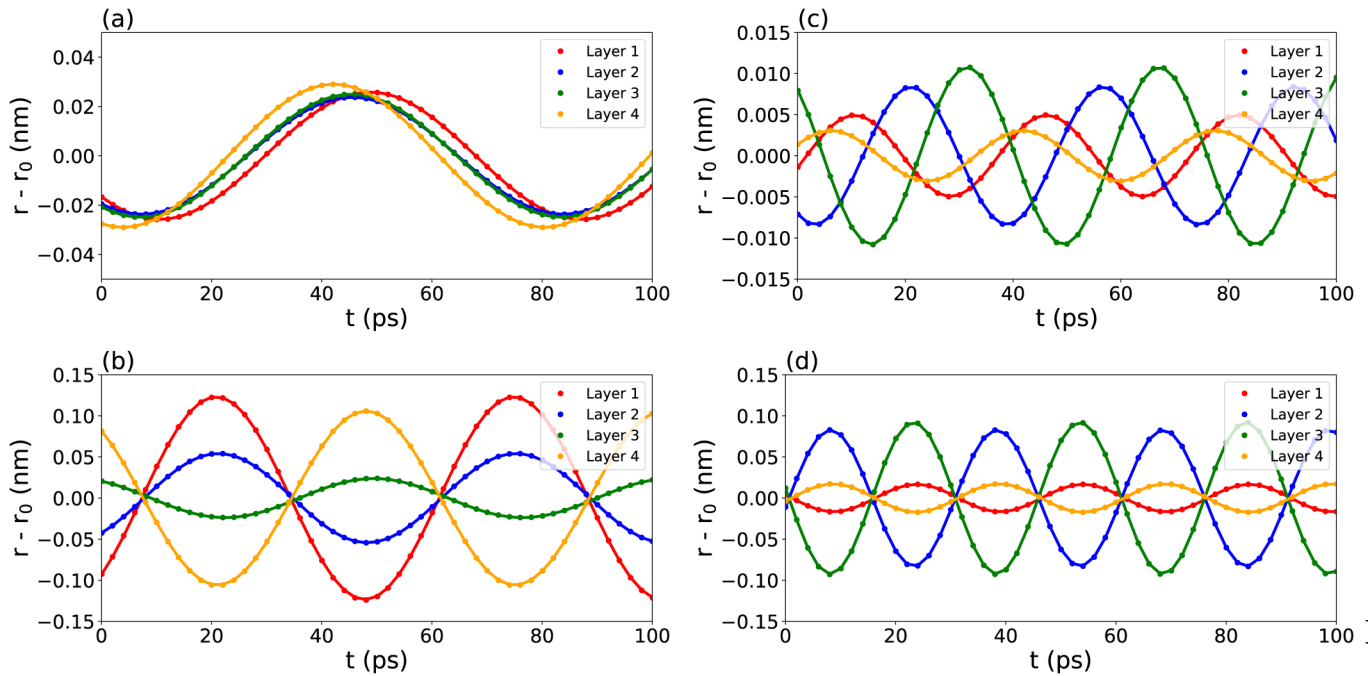


FIG. 3. (a)–(d) Real space variation of the skyrmion radius in each layer as a function of time driven at the frequencies of each of the peaks denoted in Fig. 2.

energy is minimized. The frequency splitting between the two out-of-phase modes can be understood in a similar fashion. Because of the antiferromagnetic coupling between layers, each layer is effectively screened from all but its nearest neighbors. The mode in Fig. 3(b) is only out of phase between the two central layers, while in phase between the two outer pairs of layers. Thus, the net breaking of the antiferromagnetic coupling is considerably less than for the mode in Fig. 3(d) where each skyrmion breathes out-of-phase with both the one above and below it.

This also explains the behavior shown in Fig. 4(a), which shows the frequency of the breathing modes as a function of the antiferromagnetic coupling strength σ_{RKKY} . Their frequency increases with σ_{RKKY} as we might expect as the energy barrier due to the antiferromagnetic coupling to overcome is larger. The dashed and solid lines show the corresponding frequencies of the in-phase and out-of-phase peaks found when considering a simple

SAF bilayer. As we can see the frequency of the lowest peak matches that of the bilayer skyrmion, while the two highest peaks are at a higher frequency than the out-of-phase peak. This leaves the first out-of-phase peak of our SAF multilayer, which lies at a considerably lower frequency than the equivalent in the SAF bilayer. Thus, by extending the number of layers, we are able to lower the frequency of the first observable mode as multiple arrangements become possible, including ones with lower energy than the single out-of-phase mode found in the bilayer system. We would expect this effect to scale with the number of layer repetitions and, thus, make synthetic antiferromagnetic multilayers with high numbers of repetitions the ideal media in which to observe these low frequency out-of-phase breathing modes.

Figure 4(b) shows the variation of the breathing mode frequency with the magnetic field, which varies minimally over the field range considered, despite the strong variation in skyrmion radius in Fig. 1(b). This is in contrast to the behavior in ferromagnetic systems²³ where the frequency of the breathing mode was shown to vary with the field. The only features evident at higher fields are the appearance of a trace of the in-phase breathing modes. This is as a result of the Zeeman effect discussed in Sec. III A, meaning that the disparity between the initial sizes of the skyrmions is such that a measurable frequency response can be observed. This goes to demonstrate the strong effect of the antiferromagnetic coupling on the system, dominating all other interactions. Similarly, while changing other magnetic parameters shifts the frequencies of the modes, the relation between them remains the same.

TABLE I. Relative phase in degrees of the breathing of the skyrmions in each layer when driven by a sinusoidal driving field at frequencies denoted in Fig. 2. Phases have been shifted, so the values presented are always the phase shift from layer 1.

	Peak (a)	Peak (b)	Peak (c)	Peak (d)
Layer 1	0°	0°	0°	0°
Layer 2	15.2(1)°	5.2(1)°	106.9(1)°	173.6(1)°
Layer 3	16.0(1)°	190.8(1)°	211.8(1)°	6.9(1)°
Layer 4	31.2(1)°	181.6(1)°	317.9(1)°	179.0(1)°

Downloaded from http://pubs.aip.org/aip/jap/article-pdf/doi/10.1063/5.0142772/16789097/113901_1_online.pdf

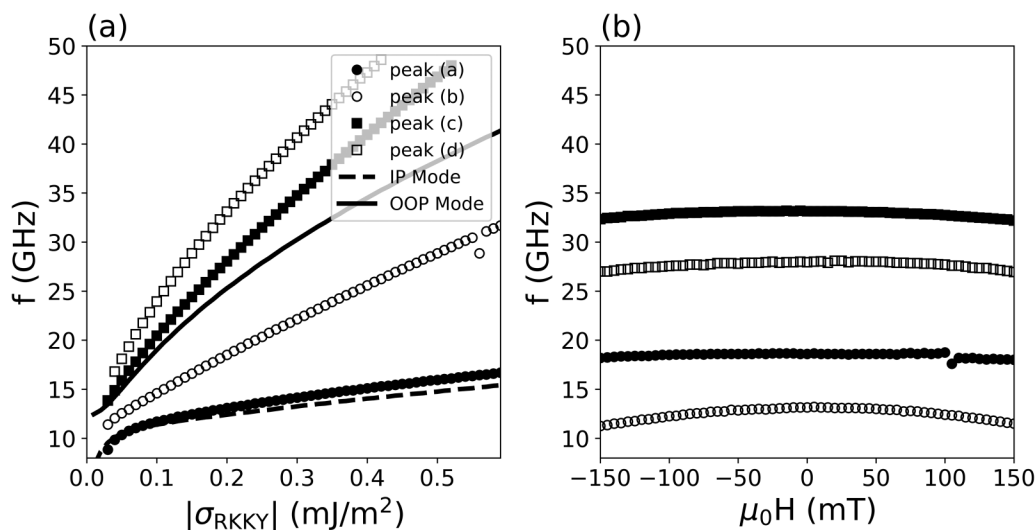


FIG. 4. (a). Peak frequencies of the SAF multilayer after the application of a sinc field pulse starting at $t = 0$ in a static field of 50 mT as a function of the antiferromagnetic coupling strength. Points show the frequencies of the peaks corresponding to panels (a)–(d) in Fig. 3, while the lines correspond to the in-phase (IP) and out-of-phase (OOP) modes for a bilayer SAF. (b). Peak frequencies as a function of the applied magnetic field with an antiferromagnetic coupling strength of -0.2 mJ/m².

C. Effects of structural disorder

While these results are fascinating as a way forward to observing the GHz response of skyrmions in a synthetic antiferromagnet, these simulations are all performed in perfectly smooth layers at zero temperature. In order to gain an insight into the effect of disorder in our systems, we performed a set of simulations with random variations in the saturation magnetization.

In typical samples grown in the lab, we would expect small variations in the thicknesses of the magnetic layers due to the effects of roughness and island-like deposition. To model this effect in our simulations, we allow the M_s of each lateral cell in our simulation to vary with a normally distributed value capped at $\pm 10\%$ of the global M_s of the system. After initializing the system with a skyrmion in the center, we allow it to relax to its equilibrium size. Then, we introduce the random variations in the M_s and allow the system to relax again. The skyrmion moves slightly to a local area of reduced free energy and otherwise does not change its size, shape, or antiferromagnetic coupling. We can then excite the disordered system with the same sinc pulse as before and use a Fourier transform to examine the frequency response of the system.

The results of comparing the disordered system to the measurements in the main manuscript are presented in Fig. 5. The frequency response of the total system is plotted in red along with the frequencies of each peak from Fig. 2 plotted as black dashed lines. We see no change in the frequency of each peak, simply a damping in the amplitudes of the peaks. The behavior of the system—arranging itself into out-of-phase detectable modes and in-phase “hidden” modes—remains the same, suggesting that such behavior would not fundamentally change in a real system. The effect of disorder on the static field-dependent behavior of skyrmions has been previously studied in Ref. 31. In this work, they use a disorder in

the M_s of comparable magnitude and show that this allows them to accurately reproduce experimental results. In addition, they show that introducing a similar disorder in any of the other micromagnetic parameters A , K , or D results in the same qualitative behavior. Thus, we believe that simply modeling the disorder of a real system by varying the M_s is a qualitatively accurate method of establishing that these modes would appear in a “real” sample.

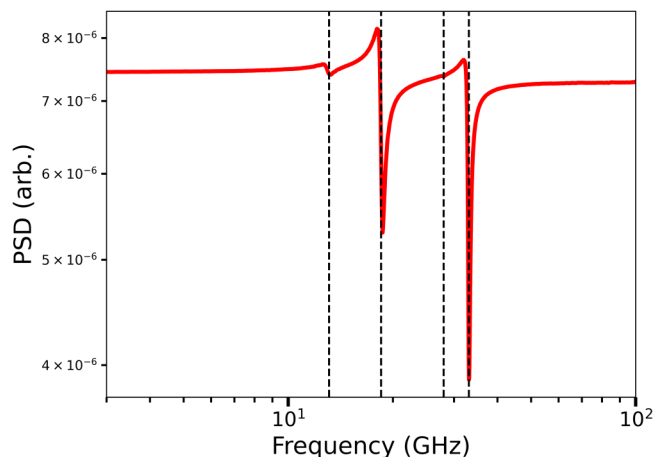


FIG. 5. Total frequency response of a four-magnetic layer SAF multilayer with disorder introduced in the M_s . Dotted lines show expected mode frequencies from Fig. 2.

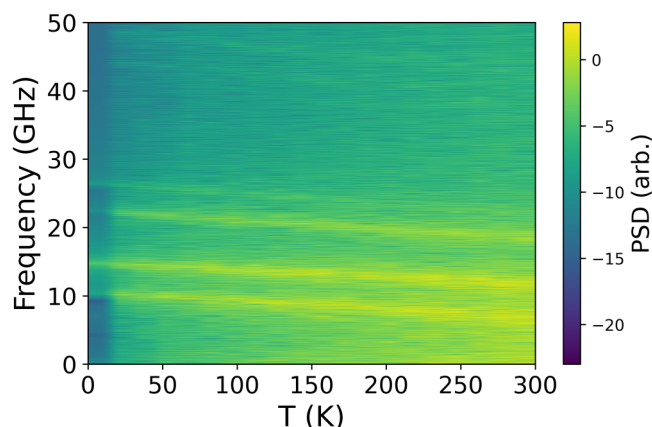


FIG. 6. Frequency of breathing modes vs temperature. Magnetization data set taken from the bottom magnetic layer in order to resolve all modes.

D. Effect of a finite temperature

In order to further examine the effects of true experimental conditions, we use the thermal field feature of `MUMAX3`²⁸ to simulate the frequency response spectrum at a range of temperatures between 0 and 300 K. The results of this are shown in Fig. 6. We see an expected decrease that appears to be close to linear in the frequency of each of the four modes with temperature and an increase in the linewidth of the peaks as well as the noise levels in the spectrum. However, the fundamental frequency relationship between modes remains unchanged, as does the number of total modes.

IV. CONCLUSION

In this work, we simulated a synthetic antiferromagnetic multilayer composed of a total of four magnetic layers, each one coupled antiferromagnetically to the one above and below it. We excite the breathing modes of the system by applying an out of plane sinc field pulse and measuring the time dependence of the total magnetization. In doing so, we find that the two modes observed in single SAFs²⁶ split further into four modes. These arrange themselves into two in-phase breathing modes and two out-of-phase breathing modes.

It has been proposed that the measurement of the microwave frequency response of skyrmions in a SAF could present a new method of skyrmion detection in an otherwise challenging system due to the negligible stray field. Our results show that in a SAF multilayer, the frequency of the first observable mode is considerably lowered in comparison with the case of a bilayer SAF. This is advantageous for observation with typically available microwave measurement apparatus, and the trend of lowered frequencies as a function of layer repetitions makes SAF multilayers with high numbers of repetitions the ideal candidate in which to observe these modes.

In addition, we are able to simulate the effects of structural and thermal disorder on our system and show that they do not have a demonstrable effect on the fundamental physics presented in the main body of our work. Realizing these measurements in

experimental conditions is difficult and has only recently been shown;²¹ however, we believe our results show that it is possible in a synthetic antiferromagnetic multilayer.

ACKNOWLEDGMENTS

The authors would like to thank J. Barker and G. Burnell for useful discussions about the work. This work was supported by EPSRC (Grant No. EP/T006803/1). C. E. A. Barker acknowledges funding from the National Physical Laboratory.

AUTHOR DECLARATIONS

Conflict of Interest

The authors have no conflicts to disclose.

Author Contributions

Christopher E. A. Barker: Conceptualization (equal); Formal analysis (equal); Investigation (equal); Methodology (equal); Writing – original draft (equal). **E. Haltz:** Conceptualization (supporting); Methodology (equal); Writing – review & editing (equal). **T. A. Moore:** Project administration (equal); Supervision (equal); Writing – review & editing (equal). **C. H. Marrows:** Conceptualization (equal); Funding acquisition (equal); Project administration (equal); Supervision (equal); Writing – review & editing (equal).

DATA AVAILABILITY

The data that support the findings of this study are openly available in the University of Leeds Data Repository at <https://doi.org/10.5518/1306>, Ref. 32.

REFERENCES

- N. Nagaosa and Y. Tokura, “Topological properties and dynamics of magnetic skyrmions,” *Nat. Nanotechnol.* **8**, 899–911 (2013).
- K. Everschor-Sitte, J. Masell, R. M. Reeve, and M. Kläui, “Perspective: Magnetic skyrmions—Overview of recent progress in an active research field,” *J. Appl. Phys.* **124**, 240901 (2018).
- S. Mühlbauer, B. Binz, F. Jonietz, C. Pfleiderer, A. Rosch, A. Neubauer, R. Georgii, and P. Böni, “Skyrmion lattice in a chiral magnet,” *Science* **323**, 915–919 (2009).
- H. Wilhelm, M. Baenitz, M. Schmidt, U. K. Rößler, A. A. Leonov, and A. N. Bogdanov, “Precursor phenomena at the magnetic ordering of the cubic helimagnet FeGe,” *Phys. Rev. Lett.* **107**, 127203 (2011).
- T. Adams, A. Chacon, M. Wagner, A. Bauer, G. Brandl, B. Pedersen, H. Berger, P. Lemmens, and C. Pfleiderer, “Long wavelength helimagnetic order and skyrmion lattice phase in Cu_2OSeO_3 ,” *Phys. Rev. Lett.* **108**, 237204 (2012).
- S. Woo, K. Litzius, B. Krüger, M. Y. Im, L. Caretta, K. Richter, M. Mann, A. Krone, R. M. Reeve, M. Weigand, P. Agrawal, I. Lemesch, M. A. Mawass, P. Fischer, M. Kläui, and G. S. Beach, “Observation of room-temperature magnetic skyrmions and their current-driven dynamics in ultrathin metallic ferromagnets,” *Nat. Mater.* **15**, 501–506 (2016).
- W. Jiang, G. Chen, K. Liu, J. Zang, S. G. te Velthuis, and A. Hoffmann, “Skyrmions in magnetic multilayers,” *Phys. Rep.* **704**, 1–49 (2017).
- R. Tomasello, E. Martinez, R. Zivieri, L. Torres, M. Carpentieri, and G. Finocchio, “A strategy for the design of skyrmion racetrack memories,” *Sci. Rep.* **4**, 1–7 (2014).

- ⁹F. Büttner, I. Limesh, and G. S. D. Beach, "Theory of isolated magnetic skyrmions: From fundamentals to room temperature applications," *Sci. Rep.* **8**, 4464 (2018).
- ¹⁰C. Back, V. Cros, H. Ebert, K. Everschor-Sitte, A. Fert, M. Garst, T. Ma, S. Mankovsky, T. L. Monchesky, M. Mostovoy, N. Nagaosa, S. S. Parkin, C. Pfleiderer, N. Reyren, A. Rosch, Y. Taguchi, Y. Tokura, K. Von Bergmann, and J. Zang, "The 2020 skyrmionics roadmap," *J. Phys. D: Appl. Phys.* **53**, 363001 (2020).
- ¹¹H. Vakili, W. Zhou, C. T. Ma, S. J. Poon, M. G. Morshed, M. N. Sakib, S. Ganguly, M. Stan, T. Q. Hartnett, P. Balachandran, J. W. Xu, Y. Quessab, A. D. Kent, K. Litzius, G. S. Beach, and A. W. Ghosh, "Skyrmionics—computing and memory technologies based on topological excitations in magnets," *J. Appl. Phys.* **130**, 070908 (2021).
- ¹²R. A. Duine, K. J. Lee, S. S. Parkin, and M. D. Stiles, "Synthetic antiferromagnetic spintronics," *Nat. Phys.* **14**, 217–219 (2018).
- ¹³X. Zhang, Y. Zhou, and M. Ezawa, "Magnetic bilayer-skyrmions without skyrmion Hall effect," *Nat. Commun.* **7**, 1–7 (2016).
- ¹⁴X. Zhang, M. Ezawa, and Y. Zhou, "Thermally stable magnetic skyrmions in multilayer synthetic antiferromagnetic racetracks," *Phys. Rev. B* **94**, 064406 (2016).
- ¹⁵W. Legrand, D. Maccariello, F. Ajejas, S. Collin, A. Vecchiola, K. Bouzehouane, N. Reyren, V. Cros, and A. Fert, "Room-temperature stabilization of antiferromagnetic skyrmions in synthetic antiferromagnets," *Nat. Mater.* **19**, 34 (2019).
- ¹⁶T. Dohi, S. DuttaGupta, S. Fukami, and H. Ohno, "Formation and current-induced motion of synthetic antiferromagnetic skyrmion bubbles," *Nat. Commun.* **10**, 5153 (2019).
- ¹⁷M. Mochizuki, "Spin-wave modes and their intense excitation effects in skyrmion crystals," *Phys. Rev. Lett.* **108**, 017601 (2012).
- ¹⁸Y. Onose, Y. Okamura, S. Seki, S. Ishiwata, and Y. Tokura, "Observation of magnetic excitations of skyrmion crystal in a helimagnetic insulator Cu_2OSeO_3 ," *Phys. Rev. Lett.* **109**, 037603 (2012).
- ¹⁹M. Mochizuki and S. Seki, "Dynamical magnetoelectric phenomena of multi-ferroic skyrmions," *J. Phys.: Cond. Matt.* **27**, 503001 (2015).
- ²⁰M. T. Birch, R. Takagi, S. Seki, M. N. Wilson, F. Kagawa, A. Štefančič, G. Balakrishnan, R. Fan, P. Steadman, C. J. Ottley, M. Crisanti, R. Cubitt, T. Lancaster, Y. Tokura, and P. D. Hatton, "Increased lifetime of metastable skyrmions by controlled doping," *Phys. Rev. B* **100**, 014425 (2019).
- ²¹B. Satywali, V. P. Kravchuk, L. Pan, M. Raju, S. He, F. Ma, A. P. Petrović, M. Garst, and C. Panagopoulos, "Microwave resonances of magnetic skyrmions in thin film multilayers," *Nat. Commun.* **12**, 1–8 (2021).
- ²²T. Srivastava, Y. Sassi, F. Ajejas, A. Vecchiola, I. Ngouagnia, H. Hurdequint, K. Bouzehouane, N. Reyren, V. Cros, T. Devolder, J.-V. Kim, and G. de Loubens, "Resonant dynamics of skyrmion lattices in thin film multilayers: Localised modes and spin wave emission," [arXiv:2111.11797](https://arxiv.org/abs/2111.11797) [cond-mat.mes-hall] (2021).
- ²³J. V. Kim, F. Garcia-Sanchez, J. Sampaio, C. Moreau-Luchaire, V. Cros, and A. Fert, "Breathing modes of confined skyrmions in ultrathin magnetic dots," *Phys. Rev. B* **90**, 064410 (2014).
- ²⁴M. Lonsky and A. Hoffmann, "Dynamic excitations of chiral magnetic textures," *APL Mater.* **8**, 100903 (2020).
- ²⁵L. Xing, D. Hua, and W. Wang, "Magnetic excitations of skyrmions in antiferromagnetic-exchange coupled disks," *J. Appl. Phys.* **124**, 123904 (2018).
- ²⁶M. Lonsky and A. Hoffmann, "Coupled skyrmion breathing modes in synthetic ferri- and antiferromagnets," *Phys. Rev. B* **102**, 104403 (2020).
- ²⁷M. Lonsky and A. Hoffmann, "Dynamic fingerprints of synthetic antiferromagnet nanostructures with interfacial Dzyaloshinskii–Moriya interaction," *J. Appl. Phys.* **132**, 043903 (2022).
- ²⁸A. Vansteenkiste, J. Leliaert, M. Dvornik, M. Helsen, F. Garcia-Sanchez, and B. Van Waeyenberge, "The design and verification of MuMax3," *AIP Adv.* **4**, 107133 (2014).
- ²⁹J. Xia, X. Zhang, K.-Y. Mak, M. Ezawa, O. A. Tretiakov, Y. Zhou, G. Zhao, and X. Liu, "Current-induced dynamics of skyrmion tubes in synthetic antiferromagnetic multilayers," *Phys. Rev. B* **103**, 174408 (2021).
- ³⁰J. Kim, J. Yang, Y. J. Cho, B. Kim, and S. K. Kim, "Coupled breathing modes in one-dimensional skyrmion lattices," *J. Appl. Phys.* **123**, 053903 (2018).
- ³¹K. Zeissler, M. Mruczkiewicz, S. Finizio, J. Raabe, P. M. Shepley, A. V. Sadovnikov, S. A. Nikitov, K. Fallon, S. McFadzean, S. McVitie, T. A. Moore, G. Burnell, and C. H. Marrows, "Pinning and hysteresis in the field dependent diameter evolution of skyrmions in Pt/Co/Ir superlattice stacks," *Sci. Rep.* **7**, 1–9 (2017).
- ³²C. E. A. Barker, E. Haltz, T. A. Moore, and C. H. Marrows (2023). "Dataset Associated with Breathing Modes of Skyrmion Strings in a Synthetic Antiferromagnet." <https://doi.org/10.5518/1306>.